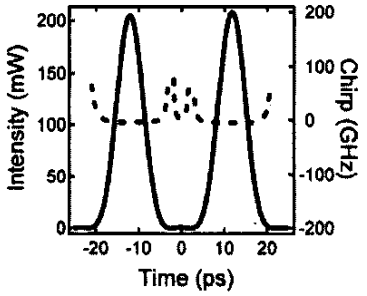

Fig. 3. Retrieved temporal intensity (solid line) and chirp (dashed line) of 40 Gbit/s pulses directly after EDFA.

The nonlinear pulse compressor consists of a length of highly nonlinear fiber (HNLF) followed by a length of standard single mode fibre (SMF). The lengths of the fibers required for the compressor were obtained from numerical simulations using the nonlinear Schrödinger equation (NLSE) and the input field obtained from the FROG measurement. The fiber parameters used in the simulation are listed in table 1.

Fiber	Loss (dB/km)	Dispersion (ps/nm/km)	Nonlinearity (/W.km)
HNLF	0.59	0.2	10.4
SMF	0.25	18.5	1.3

Table 1. Fiber parameters used in numerical model

The optimum compressor designed to compress the 7.4 ps duration 40 Gbit/s pulses to a duration of around 3.5 ps requires 1.01 km of HNLF followed by 200 m of SMF. The evolution of the pulse width as a function of propagation distance predicted by the simulation is shown in the insert to figure 1. It should be noted that whilst the minimum pulse duration of 3.2 ps is seen to occur after only 150 m the actual length of SMF chosen was 200 m. This was because the simulations showed that this gave a better compromise between pulse width and extinction ratio as further propagation in the SMF results in a reduction of the pedestal.

The 40 Gbit/s pulses were launched into the HNLF with a relatively modest average power of 18.9 dBm. The quality of the pulse compressor was characterised by carrying out FROG measurements on the compressed output pulses. Figure 4 shows the retrieved temporal intensity (circles) and chirp (squares). Also shown in figure 4 is the calculated temporal intensity (solid line) and chirp (dashed line) based on the numerical propagation of the measured input field (fig. 3) through the designed compressor. The calculated results show excellent agreement with the experimentally measured output fields. The compressed pulses have a pulse width of 3.4 ps and the extinction ratio is only slightly reduced to 21 dB.

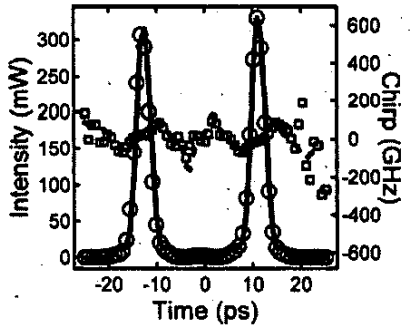

Fig. 4. Comparison between the calculated temporal intensity (solid line) and chirp (dashed line) and the experimentally measured temporal intensity (circles) and chirp (squares) of the 40 Gbit/s pulses after the fiber compressor.

In order to demonstrate the suitability of these compressed pulses for multiplexing to higher aggregate bit-rates the compressed pulses were multiplexed in a passive fiber delay line MUX to 80 Gbit/s. The temporal intensity and chirp retrieved from FROG measurements on the 80 Gbit/s pulse train are shown in figure 5. The extinction ratio after the MUX is reduced to 16 dB due to the small pedestal that is present on the compressed 40 Gbit/s pulses.

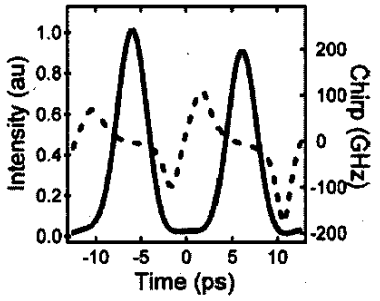

Fig. 5. Retrieved temporal intensity (solid line) and chirp (dashed line) of 80 Gbit/s pulses after the MUX.

Conclusion

The high-resolution FROG was used to optimise and characterise the 40 Gbit/s pulses generated from an externally modulated CW laser diode. The system produced 7.4 ps chirp free pulses with an extinction ratio of 23 dB that would be suitable for use in a 40 Gbit/s WDM system. The design of a nonlinear fiber compressor was greatly simplified using a numerical simulation based on the retrieved electric field from the FROG measurements. The compressor design was experimentally realized and its performance was verified using FROG measurements. The compressed pulses were 3.4 ps in duration and after multiplexing to 80 Gbit/s had an extinction ratio of 16 dB.

References

[1] Y. Zhu, *et al.*, Tech. Dig. OFC 2000, Baltimore, MD, Paper TuD4.
[2] W. S. Lee, *et al.*, Electron. Lett., vol. 36, pp. 734-736, 2000.
[3] A. Sahara, *et al.*, Tech. Dig. OFC 2001, Anaheim, CA, Paper ThF5-1.
[4] K. Suzuki, *et al.*, Tech. Dig. OFC 2001, Anaheim, CA, Paper TuN7-1.
[5] R. Trebino, *et al.*, Amer. Inst. Phys., Rev. Sci. Instrum., vol. 68, pp. 3277-3295, 1997.
[6] J. M. Dudley, *et al.*, IEEE J. Quantum Electron., vol. 35, pp. 441-450, 1999.
[7] L. P. Barry, et al., Electronics Lett., vol. 35, pp. 1166-1168, 1999.

FH7 **9:45 AM**

Nonlinear Multiplexing in Optical Fiber Communications

S. Mookherjea, A. Yariv, *Caltech, Pasadena, CA, Email: shayan@caltech.edu.*

The nonlinear evolution of a dispersion-managed soliton admits a novel nonlinear multiplexing scheme for optical communications. Information is coded onto the canonical parameters (chirp and width) characterizing the pulse.

We show that that in dispersion-managed fiber communication channels, there exists the possibility of a nonlinear multiplexing scheme, with no linear analog, that effectively multiplies the bit-rate throughput several-fold. Alternatively, we may achieve the same bit-rate while relaxing the requirements on the pulse width, so that slower modulation speeds and narrowband in-line filters may be used without paying a penalty in the information-transfer rate. In addition, the scheme is insensitive to minor variations in the multiplexing parameters. Our analysis is based on a Hamiltonian reduction of the dispersion-managed nonlinear Schrodinger equation[1], and is corroborated with direct numerical simulations.

Using the conventional soliton normalizations, Z represents the physical distance normalized by the dispersion length, T represents the physical time normalized by $T_0/1.67$ where T_0 is the full-width at half-maximum (FWHM) of the pulse envelope, $Q(Z,T)$ is the electric-field envelope normalized by the (path-averaged) peak field power, and $\sigma(Z)$ represents the periodic map of the group-velocity dispersion (GVD) coefficient (numerical values specified later). $Q(Z,T)$ evolves according to

$$\frac{\partial Q}{\partial Z}+\frac{\sigma}{2}\frac{\partial^2 Q}{\partial T^2}\pm|Q|^2 Q=\varepsilon R\,; \tag{1}$$

where $R(Z,T)$ is a complex-valued white noise process (amplitude $|\varepsilon|<<1$) characterizing the amplified spontaneous emission (ASE) noise added by the amplifiers along the transmission channel.

The envelope of the pulse, with an implicit carrier frequency and wavenumber, may be characterized as a dynamical system, fundamentally dependent on a finite set of parameters, such as pulse width (η), quadratic chirp (β), etc. Based on an ansatz for the field envelope, these parameters evolve nonlinearly as functions of the propagation distance; in certain cases, a subset of these parameters are exclusively mutually dependent and evolve in bounded closed orbits.

We use a Gaussian ansatz[1],

$$Q(Z,T)=A\sqrt{\eta}\exp\left\{-\left[\kappa\eta(T-C)^2\right]+\right.$$
$$\left.+i\Omega(T-C)+i\left[\beta\kappa^2(T-C)^2+\phi/2\right]\right\} \tag{2}$$

where A is the amplitude enhancement factor[1], κ is a number used to equate the pulse width of Eq. (1) to that of the conventional first-order soliton, C(Z) is the temporal center of the pulse in the moving reference frame (or group-velocity variation in laboratory coordinates), $\varphi(Z)$ is a phase, and $\eta(Z)$ and $\beta(Z)$ represent the width and chirp, respectively. The width and chirp of the pulse plotted at the end of each dispersion map period evolve as shown in Fig. 1. These orbits were obtained in the noiseless case ($\varepsilon=0$) from direct numerical simulation, using the split-step Fourier method. Propagation of a bitstream (envelope FWHM 16 ps) was examined over 4000 km using the following symmetric dispersion map: 22.5 km of normal-dispersion fiber with GVD coefficient -2.1 ps/(km-nm), followed by 6 km of AD fiber with GVD coefficient +17.45 ps/(km-nm), and then another 22.5 km of ND fiber with GVD coefficient -2.1 ps/(km-nm). The initial values used in this example for the outer and inner orbits were $(\eta,\beta)=(0.4,0)$ with A=1.53 and $(\eta,\beta)=(0.9,0)$ with A=1.70, respectively.

Using an ansatz Q_0 for the pulseshape in the absence of perturbations [e.g., Eq. (2)], we can form the evolution equations for the canonical parameters based on the Euler-Lagrange principle,

$$\frac{d\eta}{dZ}=-2\kappa^2\sigma\beta\eta+\varepsilon\kappa^2\frac{\eta^3}{A^2}\int dT(T-C)^2\,2\,\mathrm{Im}\left[RQ_0^*\right] \tag{3}$$

$$\frac{d\beta}{dZ}=-\frac{2\kappa}{\sqrt{\pi}}a^2A^2\eta^3+2\kappa^2\sigma(\eta^4-\beta^2)-\varepsilon\frac{\eta^3}{A^2}$$
$$\int dT\left[\frac{1}{2\eta}-2\kappa^2(T-C)^2\eta\right]2\,\mathrm{Re}\left[RQ_0^*\right] \tag{4}$$

where $\sigma(Z)$ represents the dispersion map (GVD coefficient). With $\varepsilon=0$, the above system of ODE reconstructs the phase-plane diagram shown in Fig. 1 with a high degree of accuracy[1,5].

The multiplexing scheme works as follows: the source (laser+modulator) launches a pulse with a particular combination of amplitude (width), η, and chirp, β, to place a particular pulse onto a selected trajectory, i.e., by choosing an initial value for $\eta=\eta_{\text{initial}}$ and for $\beta=\beta_{\text{initial}}$, we select the unique

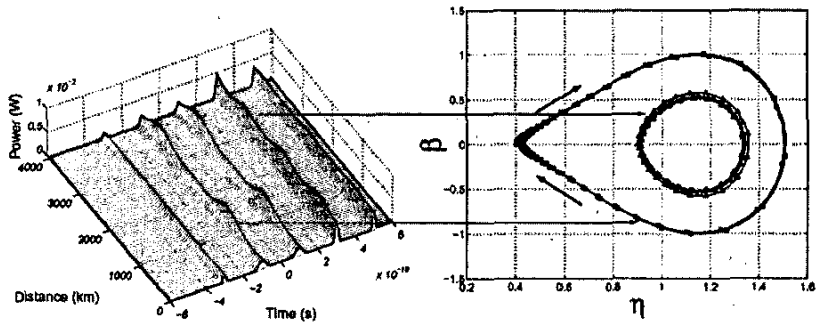

Fig. 1. Periodic orbits in the phase plane, constructed from the evolution of DM solitons over 4000 km of propagation, using direct numerical integration of the nonlinear Schrodinger equation. Two non-overlapping orbits are shown, as determined by the initial parameters of the pulse. The arrows indicate the direction of evolution.

contour that the pulse traverses as it propagates down the fiber. Different contours are assigned to the various alphabets of a multi-level code. Small variations in the initial parameters select an adjacent contour and are not of consequence if the separation between the contours assigned to different codes is chosen to be large enough (see below).

For the transmitter, a practical way of generating solitons of specific widths, especially in the picosecond regime, has been demonstrated recently by utilizing adiabatic compression in Raman amplifiers[ii]. At the receiver, straightforward techniques to distinguish between different envelope widths have been demonstrated[iii], based on the soliton self-frequency shift. [This approach has the advantage of being highly sensitive to the pulsewidth, as the frequency shift is (inversely) proportional to the fourth power of the pulsewidth.]

For example, it is practical, for current receiver technology, to require that the pulse be unchirped at the detector. In this case, there are two allowed values of $\eta=\eta_{final}$ and $\beta=\beta_{final}$ for each orbit, and the two orbits shown in Fig. 1 can implement a four-symbol multiplexing scheme, multiplying the single channel bit rate (1/inter-pulse separation) by 400%. Alternatively, we may achieve the same bit-rate while relaxing the requirements on the pulse width, so that slower modulation speeds and narrowband in-line filters may be used.

The effect of "predominantly amplified spontaneous emission (ASE) noise from the amplifiers" broadens the contours[iv] and may cause near-lying orbits to overlap. As described in detail elsewhere[v], we select orbits that are sufficiently far apart in the phase plane so that they do not overlap to the required probability of error. The parameter of interest is an effective "noise radius", which represents how "thick" the contours become, on the average, when η and β are perturbed by the stochastic noise kicks at the optical amplifiers. An analytical estimate of this noise radius may be obtained using an adiabatic variational approach[5].

Fig. 2 has been obtained directly from simulation for equally spaced amplifiers of gain 10 dB and noise figure 3 dB. In this case, four multiplexing levels are allowed, with $\eta=\eta_{final}$ and $\beta=\beta_{final}$ defined by the centers of the black circles. In this example, we have maintained the requirement that the envelopes are unchirped at the receiver in defining β_{final}. (The nonuniform density of points merely reflects that the pulse traverses the phase-plane with a non-uniform velocity.)

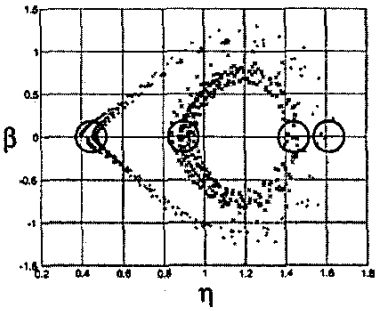

Fig. 2. Noise-induced broadening of four contours in the phase-plane. The circles, with radii defined by the "noise radius" described in the text, drawn around the points representing the received envelope $\eta=\eta_{final}$ and $\beta=\beta_{final}$ values, indicate the effective noise radius for a 10^{-9} probability of error of overlap.

If receivers can be reliably designed to detect the quadratic chirp of the received pulse, then substantially more multiplexing levels can be allowed by selecting non-overlapping neighborhoods for the parameters at the output of the channel. These neighborhoods are isomorphic to circles in R^2 or *n*-balls in R^n. The ultimate limits of such multiplexing are directly related to sphere (or ellipsoid) packing problems in *n*-dimensions, where *n* is the number of statistically significant parameters. Further, for shorter distances, more levels may be defined since the noise radii are smaller.

The authors are grateful to Dr. B. Crosignani and Dr. F. Matera for useful discussions. This work was funded by DARPA, ONR, and AFOSR..

References

i. J. N. Kutz, P. Holmes, S. G Evangelides, and J. P. Gordon. J. Opt. Soc. Am. B 15, 87 (1998).
ii. P. C. Reeves-Hall, S. A. E. Lewis, S. V. Chernikov, and J. R. Taylor. Electron. Lett. 36, 622 (2000).
iii. H. Hatami-Hanza, J. Hong, A. Atieh, P. Mylinski, and J. Chrotowski. IEEE Photon. Tech. Lett. 9, 833 (1997).
iv. J. N. Kutz and P. K. A. Wai. Opt. Lett. 23, 1022 (1998).
v. S. Mookherjea, B. Crosignani, and A. Yariv, submitted to J. Lightwave Tech. (1/2003).

FI 8:00 AM - 10:00 AM
Murphy4

Microstructure Fibers

Karl Koch, *Corning, Inc., USA, Presider*

FI1 (Invited) **8:00 AM**

"Holey" Optical Fibers: Cages for Light

J. Knight, A. Benabid, W. Reeves, T. Birks, P. Russell, *University of Bath, Bath, United Kingdom, Email: j.c.knight@bath.ac.uk.*

Optical fibers with air holes in their cross-section can deliver previously unimaginable performance. They represent an alternative fiber technology which is at a relatively early stage of development, but which can already outperform conventional fibers in certain respects.

Fibers as Cages

Conventional fiber optics relies on the use of two bulk media to form an optical waveguide, severely limiting the performance possibilities of the fibers. The limitations arise due to the optical properties of the restricted range of naturally occurring materials that have suitable mechanical and thermal properties for fiber drawing, and because of the small number of free parameters available to the fiber designer. There is another way of forming optical fibers: by microstructuring a single material. Such fibers have a long heritage [1] but have become a subject of intense activity over the past few years. The interest is due to recognition of the fantastic potential that such fibers offer, as well as the excellent progress by several groups towards recognizing this potential in different forms.

Microstructured fibers, also variously called photonic crystal fibers (PCF's) and "holey" fibers, use the very large index contrast between glass and air to influence the behavior of light in the structure. This is done by incorporating an array of holes into the fiber cross-section. This "holey" material is then used to form the cladding of an optical fiber waveguide. The pattern of holes is formed on a macroscopic scale in the fiber preform, and then reduced in transverse dimensions by several orders of magnitude while the preform is being drawn to fiber. This means that one can form features on the micron or even sub-micron scale using relatively simple fabrication procedures – they really can be "made by hand". One such procedure [2], widely used for silica PCF's, is the stack-and-draw process, in which tens or hundreds of silica capillaries are stacked together before being drawn down. Other demonstrated preform fabrication technologies include extrusion [3,4] and sol-gel casting. However the preform is created, the problem facing the fabricators remains the same: how to draw the structure down while maintaining the required uniformity and structural parameters.

In PCF, light can be confined and guided along the fiber by more than just one mechanism. One possibility is to surround a pure silica core with a lattice of air holes. These holes form the bars of a cage that traps light in guided modes in the core. The situation can be considered to be analogous to conventional fiber optics if we assign an effective refractive index to the "holey" cladding material. However, both the index and the dispersion of this effective index material are highly engineerable over a wide range. Another possible waveguiding mechanism arises if one creates a two-dimensional photonic bandgap in the cladding material. This enables one to confine light not only in a solid or liquid core, as in conventional fiber optics, but in a core comprising a gas or vacuum. Such fibers open the door to high-power transmission, because the power-handling capabilities of conventional fibers can potentially be significantly exceeded. They also promise to